DISCRETE AND CONTINUOUS
DYNAMICAL SYSTEMS SERIES B
Volume **26**, Number **1**, January **2021**

doi:10.3934/dcdsb.2020263

pp. **191–216**

CHAOTIC DYNAMICS IN A SIMPLE PREDATOR-PREY MODEL WITH DISCRETE DELAY

Guihong Fan

Department of Mathematics, Columbus State University
Columbus, Georgia 31907, USA

Gail S. K. Wolkowicz*

Department of Mathematics and Statistics, McMaster University
Hamilton, Ontario, Canada L8S 4K1, Canda

Abstract. A discrete delay is included to model the time between the capture of the prey and its conversion to viable biomass in the simplest classical Gause type predator-prey model that has equilibrium dynamics without delay. As the delay increases from zero, the coexistence equilibrium undergoes a supercritical Hopf bifurcation, two saddle-node bifurcations of limit cycles, and a cascade of period doublings, eventually leading to chaos. The resulting periodic orbits and the strange attractor resemble their counterparts for the Mackey-Glass equation. Due to the global stability of the system without delay, this complicated dynamics can be solely attributed to the introduction of the delay. Since many models include predator-prey like interactions as submodels, this study emphasizes the importance of understanding the implications of overlooking delay in such models on the reliability of the model-based predictions, especially since temperature is known to have an effect on the length of certain delays.

1. **Introduction.** A Gause type predator-prey model with response function $f(x)$ is given by

$$\begin{cases} \dot{x}(t) = rx(t)\left(1 - \dfrac{x(t)}{K}\right) - y(t)f(x(t)), \\ \dot{y}(t) = -sy(t) + Yy(t)f(x(t)), \end{cases} \tag{1}$$

where $x(t)$ denotes the density of the prey population and $y(t)$ the density of predators. Parameters r, K, s, and Y are positive constants denoting the intrinsic growth rate and the carrying capacity of the prey, the death rate of the predator in the absence of prey, and the growth yield constant for the conversion of prey to viable predator density, respectively.

If $f(x)$ is of Holling type I form in model (1) (i.e. $f(x) = mx$ where m is a positive constant denoting the maximal growth rate of the predator), it is well-known (see e.g. [2, 9]) that either the predator population approaches extinction and the prey population approaches its carrying capacity, or the predator population and the

2020 *Mathematics Subject Classification.* 34K18,34K23, 34K60, 37D45, 37G15, 37G35, 92D25, 92D40.

Key words and phrases. Predator-prey model; stage-structured model with maturation delay; Hopf and saddle-node bifurcation of limit cycles; Period doubling route to chaos; bi-stability; Mackey-Glass attractor; uniform persistence.

* Corresponding author: Gail S. K. Wolkowicz.

prey population coexist and their density approaches a positive equilibrium. Hence, for all choices of the parameters, all solutions of this system approach a globally asymptotically stable equilibrium, and so any nontrivial oscillatory behaviour that arises due to the introduction of delay in the model can be attributed solely to the delay. For this reason, we choose Holling type I response functions instead of the more realistic Holling type II form, since the Holling type II form results in a model that gives rise to nontrivial period solutions without delay (see Rosenzweig [25]). One would also expect that any exotic dynamics that the model with Holling type I form admits due to the introduction of delay would be shared by the model with Holling type II form. Li et al. [19] studied this model with the Holling type II response function of Monod form and showed that stability switches caused by varying the time delay are accompanied by bounded global Hopf branches, and they proved that when multiple Hopf branches exist, they are nested and the overlap produces coexistence of two or possibly more stable limit cycles. However, they did not go on to discover the even richer dynamics that our analysis suggests exists in that case.

Incorporating a time delay in (1) to model the time between the capture of the prey by the predator and its conversion to viable predator biomass, in the case of Holling type I functional response, $f(x) = mx$, $m > 0$, we obtain the following system:

$$\begin{cases} \dot{x}(t) = rx(t)\left(1 - \dfrac{x(t)}{K}\right) - my(t)x(t), \\ \dot{y}(t) = -sy(t) + Ye^{-s\tau}my(t-\tau)x(t-\tau). \end{cases} \tag{2}$$

The term $e^{-s\tau}y(t-\tau)$ represents those predators that survive the $\tau \geq 0$ units of time required to process the prey captured at time $t-\tau$ in the past. Thus, we have incorporated the delay in the growth term of the predator equation in a manner that is consistent with its decline rate given by the model, as described in Arino, Wang, and Wolkowicz [1].

We define $\mathbb{R}_+ \equiv \{x \in \mathbb{R} : x \geqslant 0\}$, $\text{int}\mathbb{R}_+ \equiv \{x \in \mathbb{R} : x > 0\}$. We denote by $C([-\tau, 0], \mathbb{R}_+)$, the Banach space of continuous functions from the interval $[-\tau, 0]$ into $\mathbb{R}_+$, equipped with the uniform norm. We assume initial data for model (2) is taken from

$$X = C([-\tau, 0], \mathbb{R}_+) \times C([-\tau, 0], \mathbb{R}_+). \tag{3}$$

Model (2) also has other interpretations. Gourley and Kuang [12] studied a stage-structured predator-prey model in which they included an equation for the juvenile predators and assumed a constant maturation time delay, i.e., they assumed that the juvenile predators take a fixed time to mature. Using the approach developed in Beretta and Kuang [3], the authors considered the possibility of stability switches, and concluded that there is a range of the parameter modeling the time delay for which there are periodic solutions. If the juveniles in their model suffer the same mortality rate as adult predators, their model decouples and yields model (2). Forde [8] also considered this model and conjectured that there are periodic orbits whenever the interior equilibrium exists and is unstable. He also noted that if the interior equilibrium exists and is asymptotically stable without delay, then for small delays it remains globally asymptotically stable. We show that whenever the interior equilibrium exists and is unstable, the system is uniformly persistent. Gourley and Kuang [12] had already showed that a Hopf bifurcation eventually occurs if the delay is increased, destabilizing this equilibrium and giving birth to a

nontrivial periodic solution. Forde [8] left as an open question whether more than one periodic orbit is possible and provided a numerical example suggesting chaos is possible but does not consider the route to chaos. We give numerical evidence that there is a range of parameters for which two stable periodic orbits and an unstable periodic orbit all exist and we show a period-doubling route to chaos followed by a period-halfing route back to stability of the interior equilibrium.

Cooke, Elderkin, and Huang [4] considered a model similar to the one in Gourley and Kuang [12], and obtained results concerning Hopf bifurcation of a scaled version. The scaling they used eliminated the parameter modelling the time delay, the parameter that we focus on and use as a bifurcation parameter. This simplified their analysis, since then, unlike in our case, the components of the coexistence equilibrium are independent of the time delay.

In this manuscript we show that the introduction of time delay cannot only destabilize the globally asymptotically stable coexistence equilibrium of model (2), it can also be responsible for exotic dynamics for intermediate values of the delay as well as the eventual disappearance of the coexistence equilibrium with the extinction of the predator for large enough delays. Although chaotic dynamics has been observed in other models of predator-prey interactions, the other models either require at least three trophic levels, or the response functions are not as simple and so the models admit oscillatory behavior even in the absence of delay, or the other models incorporate the delay in such a way that the predators still contribute to population growth even if the time required to process the prey is longer than the life-span of the predator (i.e., the factor $e^{-s\tau}$ is missing in the $\dot{y}$ equation), or the delay is used to model different mechanisms (see e.g., [11, 15, 24, 28]). The observation that the resulting strange attractor resembles the strange attractor for the Mackey-Glass equation [21] is also new.

This paper is organized as follows. In section 2, we scale the model and show that it is well-posed. In section 3, we consider the existence and stability of equilibria. If parameters are set so that it is possible for the predator to survive when there is no delay, it is well-known that the equilibrium at which both the prey and the predator survive is globally asymptotically stable with respect to positive initial conditions (i.e. solutions approach this equilibrium for any choice of positive initial data). In the case of delay, the components of this coexistence equilibrium depend on the delay. We prove that for positive delay, when this equilibrium exists, both the predator and the prey populations persist uniformly. However, a sufficiently long delay results in the disappearance of this equilibrium, resulting in the extinction of the predator and convergence to a globally asymptotically stable equilibrium with the prey at carrying capacity. We give criteria which when satisfied imply that there are at least two Hopf bifurcations that occur before the extinction of the predator, resulting in sustained oscillatory behaviour for intermediate values of the delay. Finally, in section 4, by means of time series, time delay embeddings, and orbit (bifurcation) diagrams we show that there are saddle-node bifurcations of limit cycles resulting in bistability as well as sequences of period doubling bifurcations leading to chaos, with a strange attractor resembling the strange attractor for the Mackey-Glass equation [21]. We conclude with a brief discussion.

2. **Scaling and basic properties of solutions.** In order to simplify the analysis, we introduce the following change of variables:

$$\begin{aligned} &\breve{t} = rt, \qquad \breve{x}(\breve{t}) = x(t)/K, \qquad \breve{y}(\breve{t}) = my(t)/r, \\ &\breve{\tau} = r\tau, \qquad \breve{s} = \frac{s}{r}, \qquad\qquad \breve{Y} = YKm/r. \end{aligned} \tag{4}$$

We drop the $\breve{}$'s for convenience and study the equivalent scaled version of model (2):

$$\begin{cases} \dot{x}(t) = x(t)(1-x(t)) - y(t)x(t), \\ \dot{y}(t) = -sy(t) + Ye^{-s\tau}y(t-\tau)x(t-\tau), \\ (x(t),y(t)) = (\phi(t),\psi(t)) \in X, \text{ for } t \in [-\tau,0], \end{cases} \tag{5}$$

where X was defined in (3).

First we address well-posedness of system (5). For positive delay τ, the existence and uniqueness of solutions of system (5) was shown in Gourley and Kuang [12]. The following proposition, proved in A.1, indicates that for positive delay the solutions remain nonnegative and provides an upper bound for each component.

Proposition 2.1. *Consider model (5) with initial data in X.*

1. *The solutions exist, are unique, and remain nonnegative for all $t \geqslant 0$.*
2. *$\limsup_{t\to\infty} x(t) \leqslant 1$ and $\limsup_{t\to\infty} y(t) \leqslant \frac{1}{4s}Ye^{-s\tau}(s+1)^2$.*
3. *Consider model (5) with initial data in X^0 where*

$$X^0 = \{(\phi(t),\psi(t)) \in X : \phi(0) > 0 \ \&\ \exists\, \theta \in [-\tau,0] \text{ s.t. } \phi(\theta)\psi(\theta) > 0\}. \tag{6}$$

Then, $x(t) > 0$ for all $t > 0$ and there exists $T \geqslant 0$ such that $y(t) > 0$ for all $t > T$.

3. **Existence and stability of equilibria and uniform persistence.** Model (5) can have up to three distinct equilibria:

$$E_0 = (0,0),\ E_1 = (1,0),\ E_+ = (x_+(\tau),y_+(\tau)) = \left(\frac{s}{Y}e^{s\tau}, 1 - \frac{s}{Y}e^{s\tau}\right). \tag{7}$$

The components of E_+ are nonnegative and E_+ is distinct from E_1, if, and only if, $0 \leqslant \tau < \tau_c$, where

$$\tau_c = \frac{1}{s}\ln\left(\frac{Y}{s}\right). \tag{8}$$

Thus, when $\tau_c > 0$, i.e., when $Y > s$, the components of E_+ are both positive, and E_+ is referred to as the coexistence equilibrium.

When there is no delay, i.e. $\tau = 0$ in (5), E_0 is always a saddle, attracting solutions with $x(0) = 0$. If $Y < s$, one of the components of E_+ is negative and so it is not relevant, and E_1 is globally asymptotically stable with respect to initial conditions satisfying $x(0) > 0$ and $y(0) \geqslant 0$. When $Y = s$, E_1 and E_+ coalesce and are globally attracting provided $x(0) > 0$. If $Y > s$, then E_1 is a saddle attracting solutions with $x(0) > 0$ and $y(0) = 0$ and E_+ sits in $\text{int}\mathbb{R}^2_+$ and is global asymptotically stable with respect to initial conditions in $\text{int}\mathbb{R}^2_+$.

When $\tau > 0$, to determine the local stability of each equilibrium solution, we use the linearization technique for differential equations with discrete delays (see Hale and Lunel [13]). After linearizing (5) about any one of these equilibria, $(x^\star, y^\star)$, the characteristic equation, $P(\lambda)|_{(x^\star,y^\star)} = 0$, is given by,

$$(\lambda+s)(\lambda+y^\star-(1-2x^\star)) + Ye^{-(s+\lambda)\tau}x^\star(1-2x^\star) - \lambda Ye^{-(s+\lambda)\tau}x^\star = 0. \tag{9}$$

We summarize the results on local and global stability of the equilibrium points and uniform persistence of the populations in the following theorem. The proof can be found in A.2.

Theorem 3.1. *Consider (5).*

1. *Equilibrium E_0 is always unstable.*
2. *Equilibrium E_1 is*
   (a) *unstable if $0 \leqslant \tau < \tau_c$, and*
   (b) *globally asymptotically stable (with respect to X^0) if $\tau > \tau_c$, (i.e. if $\frac{se^{s\tau}}{Y} > 1$).*
3. *Both components of E_+ are positive (i.e., E_+ exists), if, and only if, $0 \leqslant \tau < \tau_c$, (i.e., $\frac{se^{s\tau}}{Y} < 1$).*
   (a) *When E_+ exists and $\tau = 0$, E_+ is globally asymptotically stable with respect to $\text{int}\mathbb{R}^2_+$.*
   (b) *When E_+ exists, and $\tau \geqslant 0$, model (5) is uniformly persistent with respect to initial data in X^0, i.e., there exists $\epsilon > 0$ independent of $(\phi(t), \psi(t)) \in X^0$ such that $\liminf_{t\to\infty} x(t) > \epsilon$ and $\liminf_{t\to\infty} y(t) > \epsilon$.*

Thus, for any fixed time delay τ, if $\frac{s}{Ye^{-s\tau}} > 1$, only the prey population survives and it converges to a steady state. On the other hand, if the inequality is reversed, for appropriate initial data both the prey and the predator populations are uniformly persistent, i.e. survive indefinitely. However, we have not yet addressed what form the dynamics takes in the latter case.

3.1. **Local stability of E_+.** When E_+ exists, by Theorem 3.1 both populations survive indefinitely. To address the possible forms the dynamics can take, we begin by investigating the local stability of E_+ when it exists, i.e., when $0 \leqslant \tau < \tau_c$, and hence both components are positive. Evaluating the characteristic equation (9) at E_+ gives

$$P(\lambda)|_{E_+} = \lambda^2 + \lambda s\left(1 + \frac{e^{s\tau}}{Y}\right) + \frac{s^2}{Y}e^{s\tau} + e^{-\lambda\tau}s\left(-\lambda + \left(1 - \frac{2se^{s\tau}}{Y}\right)\right) = 0.$$

Therefore, $P(\lambda)|_{E_+} = 0$ is of the form

$$P(\lambda)|_{E_+} = \lambda^2 + p(\tau)\lambda + (q\lambda + c(\tau))e^{-\lambda\tau} + \alpha(\tau) = 0, \tag{10}$$

where

$$p(\tau) = s\left(1 + \frac{e^{s\tau}}{Y}\right), \quad q = -s, \quad c(\tau) = s\left(1 - 2\frac{se^{s\tau}}{Y}\right), \quad \text{and} \quad \alpha(\tau) = \frac{s^2e^{s\tau}}{Y}, \tag{11}$$

First assume that $\tau = 0$. Then (10) reduces to

$$\lambda^2 + (p(0) + q)\lambda + (\alpha(0) + c(0)) = 0.$$

Since $\alpha(0) + c(0) = s\left(1 - \frac{s}{Y}\right) = sy_+(0) > 0$ and $p(0) + q = \frac{se^{s\tau}}{Y} > 0$, by the Routh-Hurwitz criterion [10], all roots of (10) have negative real part. Therefore, E_+ is locally asymptotically stable when $\tau = 0$ and hence also for $\tau > 0$ sufficiently small.

We consider the stability of E_+ as τ varies in the interval $0 < \tau < \tau_c$. Here, $P(0)|_{E_+} = \alpha(\tau) + c(\tau) = s\, y_+(\tau) > 0$ and so $\lambda = 0$ is not a root of (10). Therefore, the only ways that E_+ can lose stability is: (i) when one of the characteristic roots equals zero. This only occurs when $\tau = \tau_c$. This gives rise to a transcritical bifurcation where E_+ coalesces with E_1 and then disappears as τ increases through τ_c; (ii) if characteristic roots bifurcate in from infinity; or (iii) if a pair of complex

roots with negative real parts and non-zero imaginary parts cross the imaginary axis as τ increases from 0, potentially resulting in Hopf bifurcation. In A.3 we prove that (ii) is impossible to obtain the following lemma.

Lemma 3.2. *As τ increases from zero, the number of roots of (10) with positive real part can change only if a root appears on or crosses the imaginary axis as τ varies.*

In order to determine when Hopf bifurcations occur, we first determine for what values of τ pure imaginary roots of (10) exist so that (iii) can occur. We will also be interested in secondary Hopf bifurcations.

Suppose that $\lambda = i\omega$ $(\omega > 0)$ is a root of $P(\lambda)|_{E_+} = 0$, where $i = \sqrt{-1}$. Then

$$P(i\omega)|_{E_+} = -\omega^2 + ip(\tau)\omega + (iq\omega + c(\tau))e^{-i\tau\omega} + \alpha(\tau) = 0.$$

Using Euler's identity, $e^{i\theta} = \cos\theta + i\sin\theta$, and equating the real and imaginary parts, this is equivalent to

$$\begin{aligned} c(\tau)\cos(\tau\omega) + q\omega\sin(\tau\omega) &= \omega^2 - \alpha(\tau), \\ c(\tau)\sin(\tau\omega) - q\omega\cos(\tau\omega) &= p(\tau)\omega. \end{aligned}$$

Solving for $\cos(\tau\omega)$ and $\sin(\tau\omega)$ gives

$$\sin(\tau\omega) = \frac{c(\tau)(p(\tau)\omega) + q\omega(\omega^2 - \alpha(\tau))}{c(\tau)^2 + q^2\omega^2}, \tag{12a}$$

$$\cos(\tau\omega) = \frac{c(\tau)(\omega^2 - \alpha(\tau)) + q\omega(-p(\tau)\omega)}{c(\tau)^2 + q^2\omega^2}. \tag{12b}$$

Squaring both sides of the equations in (12), adding, and rearranging gives

$$\omega^4 + (p(\tau)^2 - q^2 - 2\alpha(\tau))\omega^2 + \alpha(\tau)^2 - c(\tau)^2 = 0. \tag{13}$$

Noting that (13) is a quadratic function of ω^2, we use the quadratic formula to obtain

$$\omega_\pm^2(\tau) = \frac{1}{2}\left(q^2 - p^2(\tau) + 2\alpha(\tau) \pm \sqrt{(q^2 - p^2(\tau) + 2\alpha(\tau))^2 - 4\left(\alpha^2(\tau) - c^2(\tau)\right)}\right).$$

Substituting using (11), it follows that

$$\omega_\pm^2(\tau) = \frac{1}{2}\left(-\left(\frac{se^{s\tau}}{Y}\right)^2 \pm \sqrt{\left(\frac{se^{s\tau}}{Y}\right)^4 + s^2\left(12\frac{s^2e^{2s\tau}}{Y^2} - 16\frac{se^{s\tau}}{Y} + 4\right)}\right). \tag{14}$$

In order to determine for what values of τ there are positive real roots of (13), and hence candidates for pure imaginary roots, and possibly Hopf bifurcations, we define

$$\tau^* = \frac{1}{s}\ln\left(\frac{Y}{3s}\right). \tag{15}$$

We will prove that for $\tau \geqslant \tau^*$, there are no postive real roots and for $0 \leqslant \tau < \tau^*$

$$\omega_+(\tau) = \sqrt{\frac{1}{2}\left(-\left(\frac{se^{s\tau}}{Y}\right)^2 + \sqrt{\left(\frac{se^{s\tau}}{Y}\right)^4 + s^2\left(12\frac{s^2e^{2s\tau}}{Y^2} - 16\frac{se^{s\tau}}{Y} + 4\right)}\right)} \tag{16}$$

is the only positive real root.

Remark 1. Note that $\tau^* > 0$, if, and only if, $\frac{s}{Y} < \frac{1}{3}$, and then $x_+(\tau^*) = \frac{se^{s\tau^*}}{Y} = \frac{1}{3}$.

In the following theorem, proved in A.4, we give necessary conditions on τ for Hopf bifurcations to occur.

Theorem 3.3. *Consider (5). Assume that both components of E_+ are positive.*

1. *$\omega_+(\tau^*) = 0$. If $\tau \geqslant \tau^*$, then (13) has no positive real root. Therefore, there can be no pure imaginary roots of (10) in this case. In particular, if $\frac{s}{Y} \geqslant \frac{1}{3}$, then $\tau^* \leqslant 0$, and so there can be no Hopf bifurcation of E_+ for any $\tau \geqslant 0$.*
2. *Assume that $\frac{s}{Y} < \frac{1}{3}$, and hence, $\tau^* > 0$. If $\tau \in [0, \tau^*)$, then $x_+(\tau) \in [\frac{s}{Y}, \frac{1}{3})$, and (13) has exactly one positive real root, $\omega_+(\tau)$, given by (16). If (10) has pure imaginary roots at τ, and hence τ is a candidate for Hopf bifurcation of E_+, then $\tau \in (0, \tau^*)$ and $\omega_+(\tau)$ must satisfy (16).*

Remark 2.
1. Note that even though $\omega_+(0) > 0$ when $\frac{s}{Y} < \frac{1}{3}$, $\tau = 0$ is not a candidate for a Hopf bifurcation, since in this case all roots of (10) have negative real parts. Also, τ^* is not a candidate, since $\omega_+(\tau^*) = 0$.
2. Haque [14] finds an expression for $\omega_+(\tau^*)$ for a different scaling of the model. However, he does not go on as we do in what follows, to determine when the equations given in (12) are both simultaneously satisfied for $\omega_+(\tau^*)$, and to show that the Hopf bifurcations are nested and how the number of Hopf bifurcations increases as the death rate of the predator decreases.

Substituting the values of the coefficients given by (11), in the right-hand side of (12), and recalling that $x_+(\tau) = se^{s\tau}/Y$, we define

$$h_1(\omega, \tau) = \frac{\omega}{s}\left(\frac{s + x_+(\tau) - sx_+(\tau) - 2x_+^2(\tau) - \omega^2}{(1 - 2x_+(\tau))^2 + \omega^2}\right), \tag{17a}$$

$$h_2(\omega, \tau) = \frac{\omega^2(1 + s - x_+(\tau)) - (1 - 2x_+(\tau))sx_+(\tau)}{s\left((1 - 2x_+(\tau))^2 + \omega^2\right)}. \tag{17b}$$

Properties of the functions h_1 and h_2 are summarized in A.5.

Remark 3. By Theorem 3.3 and Lemma A.1, τ satisfies (12) for $\omega > 0$, (and hence (10) has a pair of pure imaginary eigenvalues) if and only if $\tau \in (0, \tau^*)$, and

$$\sin(\tau\omega_+(\tau)) = h_1(\omega_+(\tau), \tau), \tag{18a}$$

$$\cos(\tau\omega_+(\tau)) = h_2(\omega_+(\tau), \tau). \tag{18b}$$

Define the function

$$\theta : [0, \tau^*] \to [0, \pi] \tag{19}$$
$$\theta(\tau) := \arccos(h_2(\omega_+(\tau), \tau)).$$

By part 3 of Lemma A.1, stated and proved in A.5, $\theta(\tau)$ is a well-defined, continuously differentiable function. Replacing $\tau\omega_+(\tau)$ by $\theta(\tau) + 2n\pi$ in the left hand side of (18), we obtain

$$\sin(\theta(\tau) + 2n\pi) = h_1(\omega_+(\tau), \tau), \tag{20a}$$

$$\cos(\theta(\tau) + 2n\pi) = h_2(\omega_+(\tau), \tau). \tag{20b}$$

Equation (20b) is satisfied directly by the definition of $\theta(\tau)$. Equation (20a) is also satisfied, from parts 1 and 2 of Lemma A.1, since $0 \leqslant \theta(\tau) \leqslant \pi$.

By comparing (18) and (20), it follows that solutions of (18) occur at precisely those points where the curves $\tau\omega_+(\tau)$ and $\theta(\tau) + 2n\pi$ intersect.

Remark 4. By Remark 3, (10) has a pair of pure imaginary roots at precisely those points where the curves $\tau\omega_+(\tau)$ and $\theta(\tau) + 2n\pi$ intersect for $\tau \in (0, \tau^*)$, where n is a nonnegative integer.

For each integer $n \geqslant 0$, denote the j_n points of intersection of the curves $\tau\omega_+(\tau)$ and $\theta(\tau) + 2n\pi$ for $\tau \in (0, \tau^*)$, in increasing order, by τ_n^j, $j = 1, 2 \ldots, j_n$, i.e., for each $n = 0, 1, 2, \ldots,$

$$\tau_n^j \omega_+(\tau_n^j) = \theta(\tau_n^j) + 2n\pi, \quad j = 1, 2, \ldots, j_n.$$

Theorem 3.4. *Consider system (5). The characteristic equation (10) has a pair of pure imaginary eigenvalues, if and only if, $\tau = \tau_n^j \in (0, \tau^*)$, a point of intersection of the curves $\tau\omega_+(\tau)$ and $\theta(\tau)+2n\pi$, for some integer $n \geqslant 0$. At all such intersections, the pair of pure imaginary eigenvalues is simple and no other root of (10) is an integer multiple of $i\omega_+(\tau_n^j)$. If in addition, $\frac{\mathrm{d}}{\mathrm{d}\tau}(\tau\omega_+(\tau))\Big|_{\tau=\tau_n^j} \neq \frac{\mathrm{d}}{\mathrm{d}\tau}\theta(\tau)\Big|_{\tau=\tau_n^j}$, the transversality condition for Hopf bifurcation, $\frac{\mathrm{d}}{\mathrm{d}\tau}\mathrm{Re}(\lambda(\tau))\Big|_{\tau=\tau_n^j} \neq 0$, holds.*

The proof is given in A.6.

Remark 5. If the slope of the curve $\theta(\tau) + 2n\pi$ is less than the slope of $\tau\omega_+(\tau)$ at an intersection point τ_n^j, then a pair of complex roots of (10) crosses the imaginary axis from left to right as τ increases through τ_n^j. On the other hand, if the slope of the curve $\theta(\tau)+2n\pi$ is greater than the slope of $\tau\omega_+(\tau)$ at an intersection point τ_n^j, then a pair of complex roots of (10) crosses the imaginary axis from right to left as τ increases through τ_n^j.

Corollary 3.5. *Consider system (5). Assume that $\tau \in [0, \tau^*]$ and that there exists $N \geqslant 0$ such that $(2N + 1)\pi \leqslant \max_{\tau\in[0,\tau^*]} \tau\omega_+(\tau) \leqslant 2(N + 1)\pi$.*

1. *For $0 \leqslant n \leqslant N$, $\theta(\tau) + 2n\pi$ and $\tau\omega_+(\tau)$ have at least two intersections in $(0, \tau^*)$.*
2. *For $n \geqslant N + 1$, $\theta(\tau) + 2n\pi$ and $\tau\omega_+(\tau)$ do not intersect in $(0, \tau^*)$.*
3. *If $\theta(\tau) + 2n\pi$ and $\tau\omega_+(\tau)$ intersect for any $n \geqslant 0$, then τ_0^1 is the smallest and $\tau_0^{j_0}$ the largest value of τ for which (10) has a pair of pure imaginary eigenvalues.*
4. *The coexistence equilibrium E_+ is locally asymptotically stable for $\tau \in [0, \tau_0^1) \cup (\tau_0^{j_0}, \tau_c)$.*

The proof is given in A.7.

Our results differ from those in Gourley and Kuang [12], since we give explicit formulas for solutions of (13) and define $\theta(\tau)$ explicitly. These explicit formulas play an important role in analysis and make numerical simulations more straightforward. Although $\omega_-^2(\tau)$ in equation (14) is negative in this model and hence its square root is not real, in other models equation (13) can have two positive real solutions (see [7], where both $\omega_+(\tau)$ and $\omega_-(\tau)$ are positive). In that case, double Hopf bifurcations are possible.

In the next section we will demonstrate numerically that in the example shown in Figure 1, E_+ first loses its stability through a supercritical Hopf bifurcation as τ increases through τ_0^1 and then restabilizes as a result of a second supercritical Hopf bifurcation as τ increases through τ_0^2. We will also show that between these two values of τ there is a sequence of bifurcations resulting in interesting dynamics, including a strange attractor.

4. An example demonstrating complex dynamics.

In this section, unless specified otherwise, we select the following values for the parameters in model (2):

$$m = 1, \ r = 1, \ K = 1, Y = 0.6, \ s = 0.02, \tag{21}$$

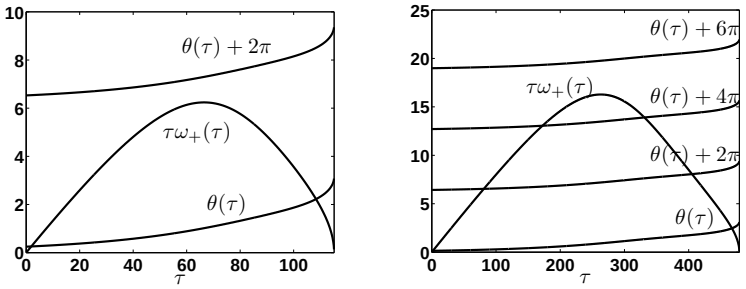

FIGURE 1. Intersections of $\theta(\tau)+2n\pi$ and $\tau\omega_+(\tau)$, $n=0,1,\ldots,$. Values of τ at which the characteristic equation has pure imaginary eigenvalues, and hence candidates for critical values of τ at which there could be Hopf bifurcations. In both graphs, at all such intersections, transversality holds, since the slope of these curves at these intersections are different. Parameters: $m=1$, $r=1$, $K=1$, $Y=0.6$. **(LEFT)** $s=0.02$. For $n=0$ there are two intersections (i.e. $j_0=2$), at τ_0^1 and τ_0^2, but for $n=1$, and hence $n\geqslant 1$, there are no intersections. **(RIGHT)** $s=0.007$. There are two intersections each (i.e. $j_n=2$, $n=0,1,2$), at τ_n^1 and τ_n^2, for $n=0,1$ and 2, but for $n=3$, and hence $n\geqslant 3$, there are no intersections. In both **(LEFT)** and **(RIGHT)**, E_+ is asymptotically stable for $\tau\in[0,\tau_0^1)\cup(\tau_0^2,\tau_c)$ and unstable for $\tau\in(\tau_0^1,\tau_0^2)$.

and consider τ as a bifurcation parameter. Since, with this selection of parameters, the model is already in the form of the scaled version of the model (5), it is not necessary to apply the scaling given by (4). We first use this example to illustrate the analytic results given in section 3 where we provided necessary and sufficient conditions for a simple pair of pure imaginary eigenvalues of the characteristic equation to occur as τ varies. We then provide bifurcation diagrams with τ as the bifurcation parameter, simulations including time series and time delay embeddings for various values of τ, and a return map at a value of τ at which there is a chaotic attractor, in order to illustrate the wide variety of dynamics displayed by the model, even in the case when there are only two Hopf bifurcations. This includes two supercritical Hopf bifurcations, saddle-node bifurcations of limit cycles and sequences of period doublings that appear to lead to chaotic dynamics with a strange attractor reminiscent of the strange attractor for the well-known Mackey-Glass equation [20, 21]

$$\frac{dx}{dt}=\beta\frac{x(t-\tau)}{1+(x(t-\tau))^n}-\gamma x(t).$$

4.1. **Illustration of analytic results.** For the parameters given by (21), the model has three equilibria: $E_0=(0,0)$, $E_1=(1,0)$, that always exist, and $E_+=(x_+(\tau),y_+(\tau))=(0.0\dot{3}e^{0.02\tau},1-0.0\dot{3}e^{0.02\tau})$, given by (7). The components of E_+ are both positive, if, and only if, $\tau\in[0,\tau_c)$, where $\tau_c\approx 170$ (see (8)), and by part 3(b) of Theorem 3.1 the model is uniformly persistent for $\tau\in[0,170)$.

E_0 is always a saddle, and hence unstable. E_1 is globally asymptotically stable for $\tau>\tau_c$, and unstable for $\tau\in[0,\tau_c)$. For $\tau=0$, E_+ is asymptotically stable, and by Lemma 3.2, can only lose stability by means of a Hopf bifurcation. In

order to determine the critical values of τ at which there is a pair of pure imaginary eigenvalues: $\lambda(\tau) = \pm i\omega(\tau)$, we consider the interval $(0, 115)$, since by Theorem 3.3, the interval on which $\omega(\tau)$ is positive, is bounded above by $\tau^* \approx 115$ (defined in (15)).

With the parameters given in (21), by (16) the function

$$\omega_+(\tau) = \sqrt{-.\dot{5}\ 10^{-3}(e^{0.02\tau})^2 + \frac{\sqrt{1.235\ 10^{-6}(e^{0.02\tau})^4 + .5\dot{3}\ 10^{-5}e^{0.04\tau} - 0.5\dot{3}e^{0.02\tau} + 4}}{2}}$$

and recall, by (19)

$$\theta(\tau) = \arccos(\cos(\tau\omega_+(\tau))).$$

The intersections of the functions $\tau\omega_+(\tau)$ and $\theta(\tau) + 2n\pi$, n a nonnegative integer, in the interval $(0, \tau^*)$, give the critical values of τ for which there is a pair of pure imaginary eigenvalues. There are only two intersections as can be seen in Figure 1 **(LEFT)**. Since, $\pi < \max_{\tau\in[0,\tau^*]} \tau\omega(\tau) < 2\pi$, by Corollary 3.5, we are guaranteed at least two values of $\tau > 0$ at which the characteristic equation has a pair of pure imaginary roots. In fact, (see Figure 1 ((LEFT)), there are precisely two such values, τ_0^1 and τ_0^2. Using Maple [22], we found that $\tau_0^1 \approx 1.917$ and $\tau_0^2 \approx 108.365$. By Theorem 3.4, the slopes of the curves $\theta(\tau)$ and $\tau\omega_+(\tau)$ are different at these intersection points, since these curves cross transversally (see Figure 1 (LEFT)), and hence the transversality required for Hopf bifurcation holds at each root. By part 4 of Corollary 3.5 and Remark 5, the stability of E_+ changes from asymptotically stable to unstable as τ increases through τ_0^1 and from unstable to asymptotically stable as τ increases through τ_0^2, and is unstable for $\tau \in (\tau_0^1, \tau_0^2)$. But recall, even though E_+ is unstable here, by part 3(b) of Theorem 3.1, the model is still uniformly persistent in this interval.

Thus, we have shown that for the parameters chosen, there are exactly two candidates for Hopf bifurcations (see [26], Chapter 6, Theorem 6.1, page 89-90). That both Hopf bifurcations are supercritical (involving first the birth, and then the disappearance of orbitally asymptotically stable periodic solutions) will be demonstrated in the next section. As τ increases through $\tau = 1.917$, a family of orbitally asymptotically stable periodic orbits is born. We will see that these periodic orbits undergo additional bifurcations as τ increases, and that they disappear when τ increases through the critical value $\tau = 108.365$, at the second supercritical Hopf bifurcation.

By decreasing s, the value of n for which the curves $\theta(\tau) + 2n\pi$ and $\tau\omega_+(\tau)$ intersect can increase. See Figure 1 (RIGHT) for an example with $s = 0.007$ for which the curves $\theta(\tau) + 2n\pi$ and $\tau\omega_+(\tau)$ intersect when $n = 0, 1, 2$. In fact, there are 6 points of intersection. We see by Remark 5, that for this example, E_+ is asymptotically stable until $\tau = \tau_0^1$, is unstable for $\tau \in (\tau_0^1, \tau_0^2)$, and finally becomes stable again for $\tau \in (\tau_0^2, \tau_c)$. Again, even though the model is unstable for $\tau \in (\tau_0^1, \tau_0^2)$, by part 3(b) of Theorem 3.1, it is uniformly persistent in this interval, since the model is uniformly persistent whenever both components of E_+ are positive, i.e., for $\tau \in [0, \tau_c)$.

4.2. **Saddle-node of limit cycles, period doublings, and chaotic dynamics.** The computations and figures in this section were done using Maple [22], MATLAB [23], and XPPAUT [6]

In Figure 2 (TOP), for each value of $\tau \in [0, 120]$, starting with initial data $x(t) = y(t) = 0.1$ for $t \in [-\tau, 0]$, we integrate long enough for the solution to converge to an

attractor (e.g., equilibrium, periodic orbit, or strange attractor), and then plot the local minima and maxima of the $y(t)$ coordinate on the attractor. Because we are interested in period doubling bifurcations, we then eliminate certain local maxima and minima that are due to kinks in the solutions (see Figure 3) rather than actual bifurcations, to obtain the graph in Figure 2 (BOTTOM)). Our solutions have kinks for values of $\tau \in [55, 98]$. Kinks were also observed in the Mackey-Glass equation [21].

Figure 2 confirms that there are two Hopf bifurcations at $\tau \approx 1.917$ and $\tau \approx 108.365$, and allows us to conclude that these Hopf bifurcations are both supercritical, since they involve a family of orbitally asymptotically stable periodic orbits.

Next we focus on the more interesting dynamics observed for $\tau \in [80, 100]$ (see Figure 4). There appears to be a discontinuity in the bifurcation diagram for $\tau \approx 82.225$. Upon further investigation we have determined that there is a saddle-node bifurcation of limit cycles at this value of τ and another saddle-node bifurcation of limit cycles for a value of τ smaller than $\tau = 81$. For values of τ between these two saddle-node bifurcations, there is bistability. There are two orbitally asymptotically stable period orbits. An example of two such orbits is given in Figure 5, where $\tau = 81$.

Figure 4 suggests that there are sequences of period doubling bifurcations, one initiating from the left at $\tau \approx 83$, 86, 86.6, ..., and one initiating from the right at $\tau \approx 98.3$, 93.2, 92.2, and τ between 92 and 91.85. To demonstrate these sequences, time series ($y(t)$ versus t) and time delay embeddings ($y(t)$ versus $y(t-\tau)$) at values of τ between these bifurcations are shown in Figures 6 and 7.

Figure 4 also suggests that between these sequences of period doubling bifurcations there is a window of values of τ at which there are periodic attractors that do not have a period that results from a bifurcation with period approximately equal to 2^n for some integer n, and there is chaotic dynamics. An example of the former is illustrated in Figure 8. For $\tau = 90.7$, the time-series embedding of a periodic orbit with period approximately equal to 1800 time steps involving six loops (2 times 3) is shown.

The time series and the time delay embedding of a chaotic attractor for $\tau = 90$ is shown in Figure 9. The projection of this attractor into $(x(t), y(t))$-space is also shown in Figure 10. This strange attractor resembles the chaotic attractor of the well-known Mackey-Glass equation ([21], Figure 2). The return map shown in Figure 11, for $\tau = 90$, also resembles the return map for the Mackey-Glass equation ([21], Figure 14) in the case of chaotic dynamics. Sensitivity to initial data is a hallmark of chaotic dynamics. Figure 12**(RIGHT)** demonstrates that there is sensitivity to initial data in the case of the solution for $\tau = 90$ that converges to the strange attractor, shown in Figure 9. To show that this is not just a numerical artifact, in Figure 12**(LEFT)** we show that, as expected, there is no sensitivity for the solution for $\tau = 92$ that converges to the periodic solution shown in Figure 7.

This example demonstrates that including delay in a simple predator-prey model that always has a globally asymptotically stable equilibrium point in the absence of delay, cannot only destabilize a globally asymptotically stable equilibrium point, but can even result in the birth of a strange attractor.

5. Discussion and conclusions.

We investigated the effect of the time required for predators to process their prey on the possible dynamics predicted by a mathematical model of predator-prey interaction. We incorporated a discrete delay to

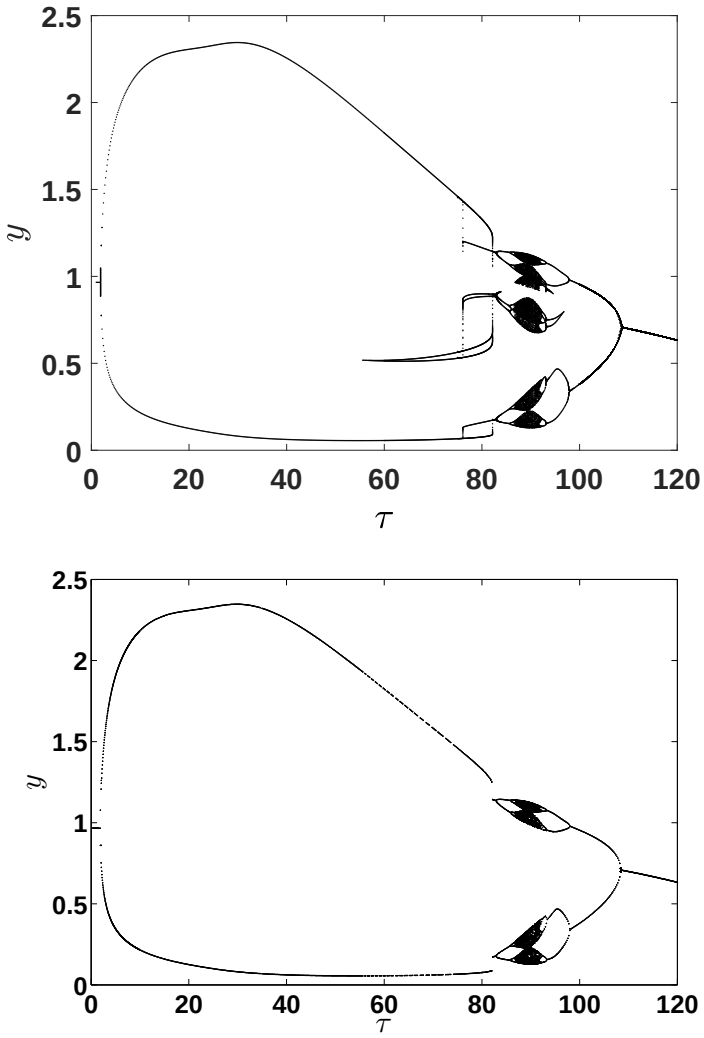

FIGURE 2. Orbit diagrams. Initial data was taken to be $x(t) = y(t) = 0.1$ for $t \in [-\tau, 0]$. However, we found bistability in the portion of the diagram beween the vertical dots and varied the initial data as explained below. Except for the portion between the vertical dots, the rest of the diagram was the same for all of the initial conditions we tried (not shown). **(TOP)** All local maxima and minima for the $y(t)$ coordinate of the attractor as τ varies, including kinks. **(BOTTOM)** Diagram including local maxes and mins for the $y(t)$ coordinate as τ varies, but with kinks eliminated. There are two saddle-node of limit cycle bifurcations. They occur for τ approximately equal to 76 and 82, where the curves in the orbit diagrams stop abruptly and there appear to be vertical dots. For τ between these values, there is is bistability. Two orbitally asymptotically stable periodic orbits (with their maximum and minimum amplitudes shown) and an unstable periodic orbit with amplitudes between them (not shown). The two stable periodic orbits were found by producing this part of the orbit diagram varying τ forward and then varying it backwards but startng at the last point of the attractor for the previous value of τ.

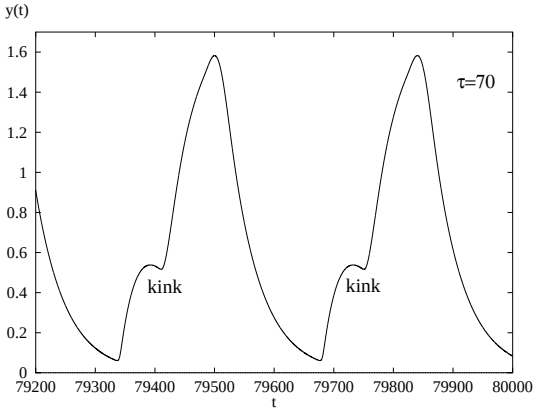

FIGURE 3. The time series for $y(t)$ when $\tau = 70$, depicting kinks. There are two local maxima and two local minima over each period as shown in Figure 2 (TOP), but only one local maxima and one local minima in Figure 2 (BOTTOM) in which kinks have been removed.

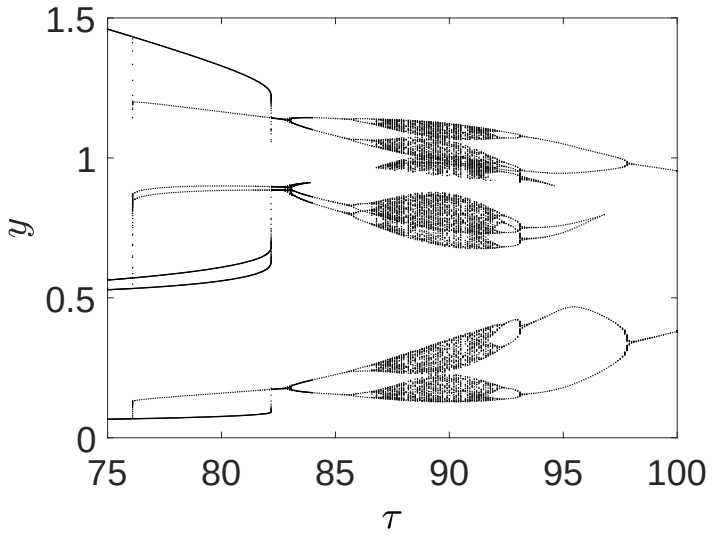

FIGURE 4. Zoom-in of orbit diagram shown in Figure 2 for $\tau \in [75, 100]$ including kinks. The vertical dots indicate the boundary of the region of bistability, where the two saddle-node of limit cycle bifurcations occur.

model this process in one of the simplest classical predator-prey models, one that only allows convergence to an equilibrium when this delay is ignored. We showed that including the delay results in a model with much richer dynamics. By choosing one of the simplest models when delay is ignored, one that predicts that no oscillatory behaviour is possible, the effect of the delay on the dynamics is emphasized.

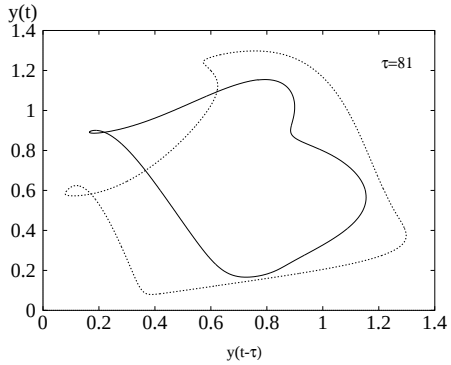

FIGURE 5. Time delay embedding of two orbitally asymptotically stable periodic orbits demonstrating bistability for $\tau = 81$. The one with larger amplitude (dashed) has initial data $x(t) = y(t) = 0.1$, for $t \in [-\tau, 0]$, and period approximately 345. The one with smaller amplitude (solid) has initial data $x(t) = y(t) = 0.1$, for $t \in [-\tau, 0)$ and $x(0) = 0.3,\ y(0) = 0.83$ and has period approximately 273.7.

This model can also be interpreted as a model of a stage-structured population with the delay modelling the maturation time of the juveniles (see Gourley and Kuang [12]).

In the model we considered, the prey are assumed to grow logistically in the absence of the predator. The interaction of the predator and prey is described using a linear response function, often referred to as mass action or Holling type I. It is well-known that when delay is ignored this is one of the simplest predator-prey models for which all solutions converge to a globally asymptotically stable equilibrium point for all choices of the parameters. Therefore, any resulting non-equilibrium dynamics would then be solely attributable to the introduction of the delay in the growth term of the predator. We not only found non-trivial periodic solutions, but also bistability, and chaotic dynamics. It is then likely that there is similar rich dynamics in most predator-prey models with any reasonable response function, when such a delay is incorporated, for some selection of the parameters, including the form most used by ecologists, the Holling type II form. This form given mathematically by $f(x) = mx/(1+bx)$), can be considered a generalization of the Holling type I form, obtained by simply adding an extra parameter, b. However, we feel that demonstrating that this wide range of dynamics is possible even for one of the simplest models gives more compelling evidence that delay should not be ignored when making policy decisions.

Understanding how changes in average temperature might affect survivability of endangered populations or result in invasions by undesirable populations is important. Since temperature can affect how quickly predators process the prey that they capture, based on our results there might be important implications for populations in the wild. In most predator populations, the processing time, τ, is faster when it is warmer and slower when it is colder. Our results may help us understand how a change in average temperature might influence the dynamics of particular predator-prey systems of interest.

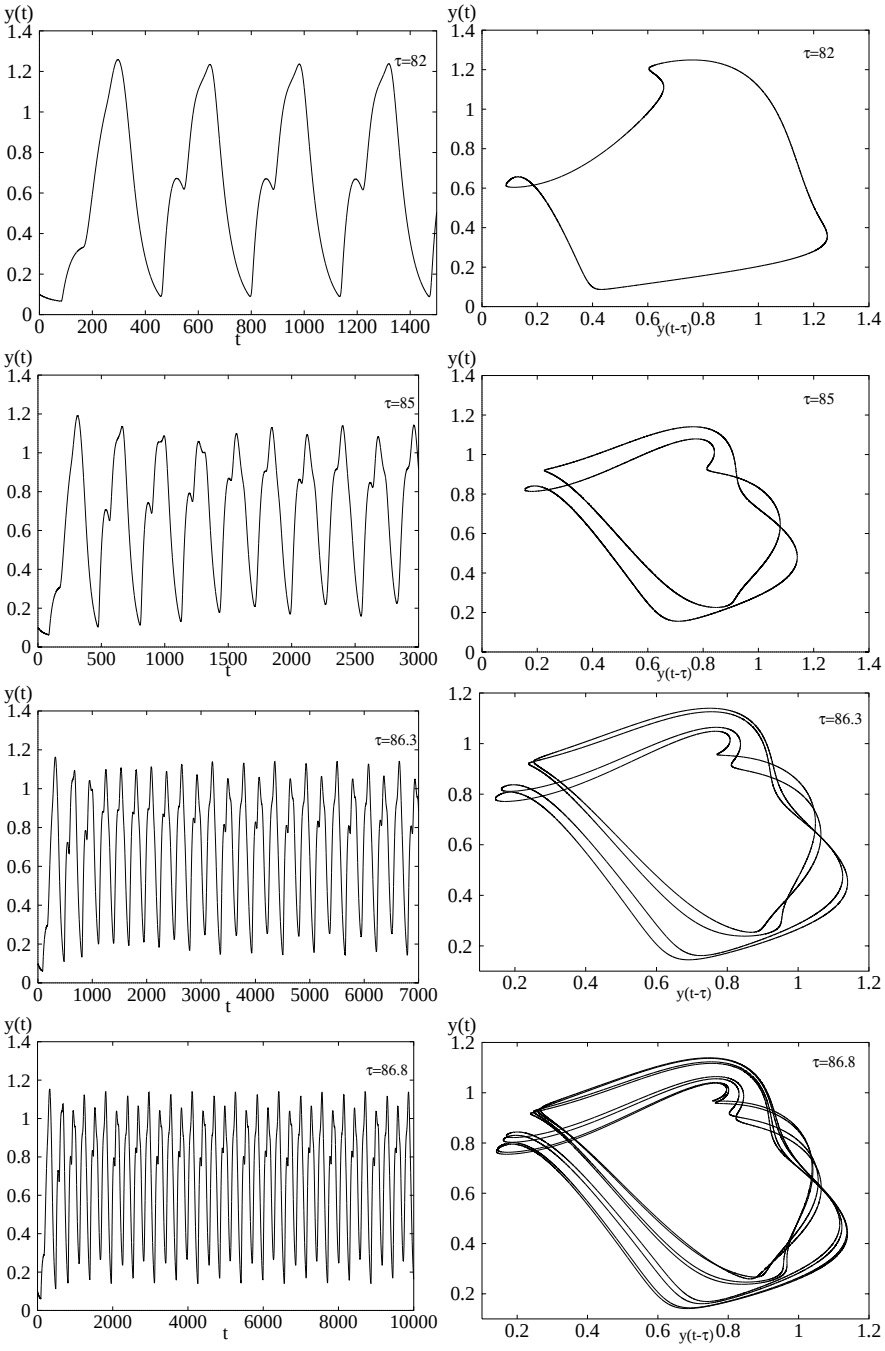

FIGURE 6. **(LEFT)** Time series starting from the initial data $x(t) = y(t) = 0.1, t \in [-\tau, 0]$ indicating how quickly the orbit gets close to the periodic attractor and **(RIGHT)** time delay embeddings of the periodic attractors, demonstrating the sequence of period doubling bifurcations initiating from the left at $\tau \approx 83,\ 86$, and 86.6. Values of τ selected between these bifurcations: $\tau = 82,\ 85,\ 86.3$, and 86.8, with periods of the periodic attractor approximately equal to: 340.2, 564.6, 1144.5, and 2298.3, respectively, are shown.

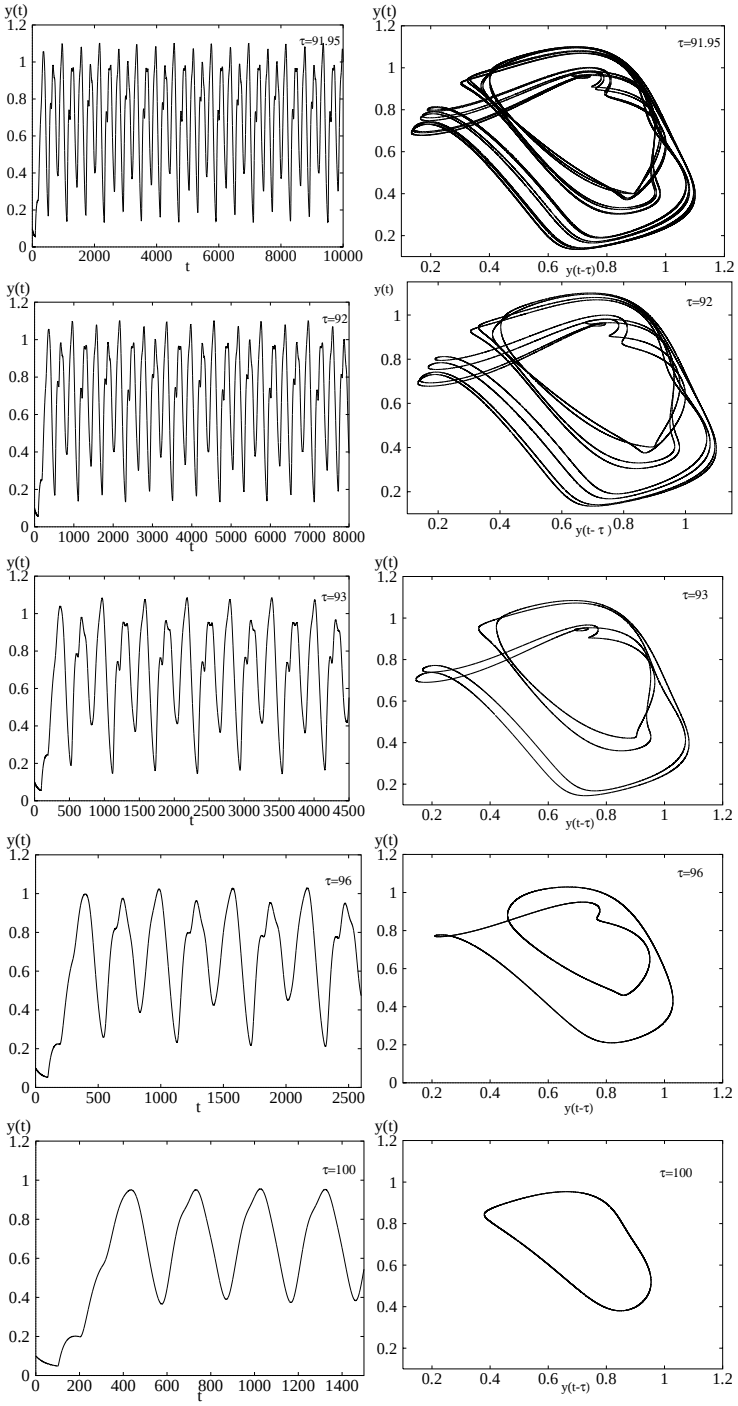

FIGURE 7. **(LEFT)** Time series starting from the initial data $x(t) = y(t) = 0.1, t \in [-\tau, 0]$ indicating how quickly the orbit gets close to the periodic attractor and **(RIGHT)** time delay embeddings of the periodic attractors, demonstrating the sequence of period halfing bifurcations initiating from the left for values of τ between 91.5 and 92, and at $\tau \approx 92.2,\ 93.2,\ 98.3$. Graphs shown are for values of τ between these bifurcations: $\tau = 91.95,\ 92,\ 93,\ 96,$ and $100,$ with periods approximately equal to: 4794.3, 2398.3, 1211.2, 557.6, and 295.3, respectively.

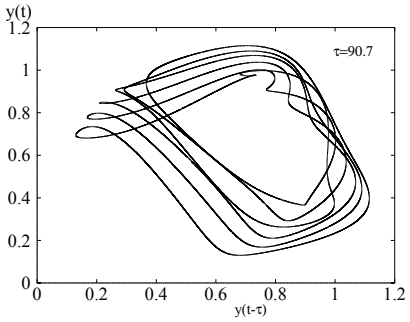

FIGURE 8. Time delay embedding starting at initial data $x(t) = y(t) = 0.1, t \in [\tau, 0]$ for $\tau = 90.7$ showing a periodic attractor with period approximately 1800, having $6 (\neq 2^n)$ loops for some integer n.

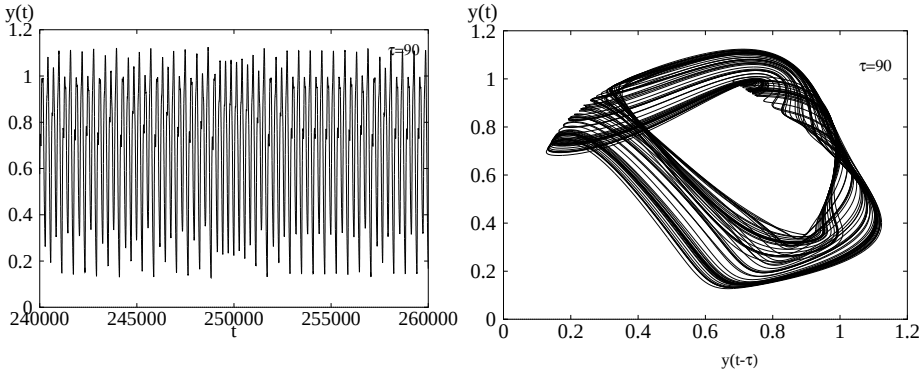

FIGURE 9. **(LEFT)** Time series for $\tau = 90$ starting from the initial data $x(t) = y(t) = 0.1, t \in [-\tau, 0]$. **(RIGHT)** Time delay embedding of the strange attractor for $\tau = 90$. Only the portion of the orbit from $t = 240,000 - 260,000$ is shown.

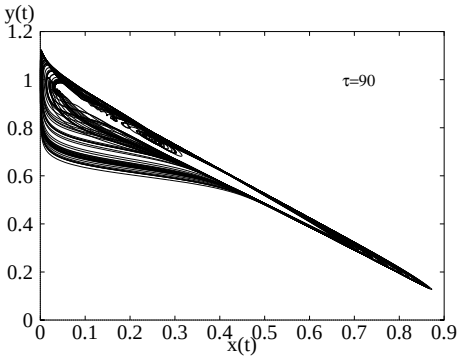

FIGURE 10. The strange attractor, for $\tau = 90$, shown in Figure 9 in (x, y)-space. Only the portion of the orbit from $t = 240,000$ to $260,000$ is shown.

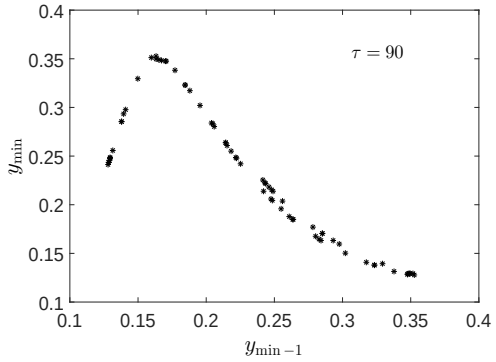

FIGURE 11. The return map for $\tau = 90$, computing the minimum value of $y(t)$ as a function of the preceding minimum value of $y(t)$ for $y(t) < 0.7$ in both cases, using the data in Figure 9.

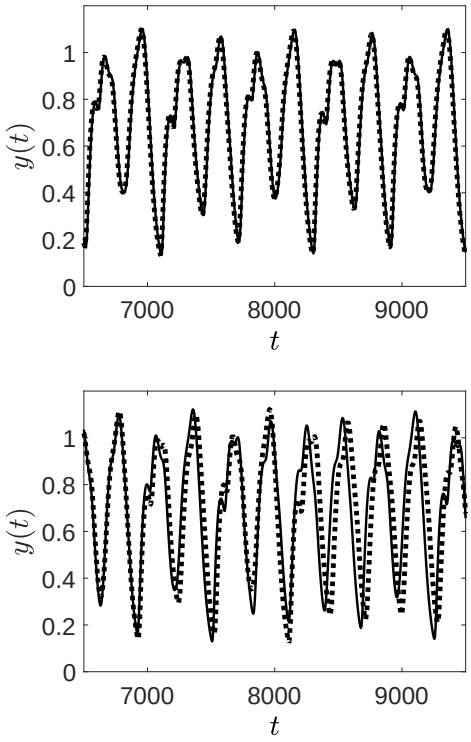

FIGURE 12. Time series **(LEFT)** for the solution that converges to a periodic attractor when $\tau = 92$, and **(RIGHT)** for the solution that converges to a strange attractor when $\tau = 90$, demonstrating that there is no sensitivity to initial data in the former case, but that there is sensitivity in the latter case. Initial data used for the solid curves: $x(t) = y(t) = 0.1$ for $t \in [-\tau, 0]$, and for the dotted curves: $x(t) = 0.11$ and $y(t) = 0.1$ for $t \in [\tau, 0]$.

Our study suggests that we need to be careful when measuring population sizes in the wild and predicting the general health of the population based upon whether the population seems to be increasing or decreasing. Short term indications that a population size is changing in a system with oscillatory dynamics may be misleading and predicting future population size may be impossible without more information. It would be necessary to have some idea of the period of the intrinsic oscillations if the population is suspected to vary periodically. If the dynamics are suspected to be chaotic, this may be even more complicated, due to sensitivity to initial data.

If a predator-prey system has the potential to have chaotic dynamics, based on our results, is there anything that is predictable? Can such analyses suggest how to prevent extinctions or invasions due to a change in average temperature that could result in a change in the processing time of the prey by the predator? We give some observations based on the predictions of our model and the example we considered in Section 4. However, more work would need to be done to determine whether these predictions are consistent for more realistic models, and if so, long term observations would have to be made by ecologists to determine if they are relevant for populations in the wild.

First, at the one extreme, if the processing time is too long, the predator population would not be expected to survive, since it is obvious that if the processing time is longer than the life span of the predator, the predator population has no chance to avoid extinction. If there was no such threshold for extinction predicted by the model, the model should be abandoned. It is therefore very important to use the term $e^{-s\tau}y(t-\tau)$ and not just $y(t-\tau)$ in order to account for the predators that do not survive long enough to affect growth of the population, in the equation describing the growth of the predator in model (2). Due to this term, in our model there is such a threshold, τ_c.

From the orbit diagram (see Figure 2), for the example considered in Section 4, we summarize some observations. The dynamics for both populations are oscillatory for a wide range of processing times, and non-oscillatory for only relatively (very) short or relatively long processing times (i.e. before the first Hopf bifurcation at $\tau \approx 1.9$ and after the last one at $\tau \approx 108$). For relatively long processing times, slightly larger than the value of τ at the final Hopf bifurcation of the coexistence equilibrium, the population is no longer oscillatory. The size of the predator population decreases relatively slowly as the processing time increases further. Although the size of the predator population gets smaller as the processing time increases, it does not get much smaller, until the processing time gets close to the threshold for extinction τ_c. If we had shown the diagram extended to the threshold $\tau_c = 170$, one would see that as the processing time gets close to τ_c, the size of the predator population suddenly decreases relatively quickly to zero. So our model predicts that for a predator population with fairly long processing times to begin with, cooling of the environment could be expected to be detrimental with respect to the survivability of the predator population. Thus, this effect on the size of the predator population might be minor if the delay is close to its Hopf bifurcation value, but could be drastic if it is close to the extinction value.

Our example also suggests that the predator population may not be oscillatory when it becomes endangered and hence close to extinction, i.e., for excessively long processing times. It would be interesting to investigate if this also holds for the model, with Holling type I response functions replaced by Holling type II. In the model with Holling type II response functions, if the carrying capacity of the

environment for the prey is not affected by the cooling and it is relatively high, then the model predicts that the predator population could still be oscillatory, even if the processing time for the predator is ignored. However, cooling might also be expected to reduce the carrying capacity for the prey, moving the parameters to a range where that model would also predict non-oscillatory dynamics (the paradox of enrichment [25]). So once again, perhaps alarm bells should be sounded when there is cooling and the predator population has been non-oscillatory and appears to decline rapidly as the average yearly temperature declines.

On the other hand, at the other extreme, our model predicts a Hopf bifurcation at a relatively small value of the delay, resulting in the birth of a family of periodic orbits with amplitude increasing very quickly as the delay increases with both the prey and predator populations spending time very close to zero. This remains the case for small, but intermediate values of the delay, (before the two saddle node of limit cycles bifurcations near $\tau = 80$). For this range of τ, these populations are therefore very susceptible to stochastic extinctions. If the processing time was originally very small (below the critical value for the first Hopf bifurcation) and cooling made it longer, again a stochastic extinction might be likely. Similarly, if τ was close to the first of the two saddle node of limit cycles bifurcations near $\tau = 80$), warming of the average temperature could result in a stochastic extinction of one or both of the populations. Since the predator cannot survive without the prey in our model, even if it was the prey population that experienced the stochastic extinction, the predator population would eventually die out as well. Between the smallest value of τ at which there is a period doubling bifurcation, and the value of τ at the largest Hopf bifurcation, cooling would probably be advantageous to the predator population size.

In summary, it seems that whether cooling is beneficial or detrimental to the size of the predator population depends on where the delay is on the bifurcation diagram, and it is very likely that this is very difficult to determine. As well, if values of τ were to lie in the chaotic region, then changes in the environment that changed the value of τ to obtain regular oscillatory dynamics may or may not be preferable. As well, as can be seen by the various attractors shown in Figures 6-10, and the orbit diagrams in Figure 4, certain properties of the system in the chaotic region such as the maximum and minimum values of the predator size were fairly insensitive to the change in the delay. This is only a toy model. However, it suggests that ignoring delay in a model can result in incorrect predictions. Here, delay could change the dynamics from convergence to a globally asymptotically stable equilibrium to wild oscillations. It is most likely that in nature, it would not be possible to distinguish from data, a priori, if the dynamics were chaotic or periodic, but more importantly it would not necessarily be predictable what the effect of an increase or a decrease in the delay would be. Hence, our analysis indicates that one should be extra cautious if trying to manipulate the delay to achieve a certain result based on model predictions.

Finally it is worth pointing out that the resulting strange attractor in the predator-prey model studied here bares such a close resemblance to the Mackey-Glass attractor, a model involving a single delay differential equation to model a simple feedback system for respiratory control or hematopoietic diseases. Understanding whether there is a deeper significiance to this relationship may give us a better understanding of the class of possible strange attractors and warrants further investigation.

Funding. The Research of Gail S. K. Wolkowicz was partially supported by Natural Sciences and Engineering (NSERC) Discovery Grant # 9358 and Accelerator supplement.

REFERENCES

[1] J. Arino, L. Wang and G. S. K. Wolkowicz, An alternative formulation for a delayed logistic equation, *J. Theoret. Biol.*, **241** (2006), 109–119.
[2] A. D. Bazykin, *Nonlinear Dynamics of Interacting Populations*, vol. 11 of A, World Scientific Series on Nonlinear Science, Singapore, 1998.
[3] E. Beretta and Y. Kuang, Geometric stability switch criteria in delay differential systems with delay dependent parameters, *SIAM J. Math. Anal.*, **33** (2002), 1144–1165.
[4] K. L. Cooke, R. H. Elderkin and W. Huang, Predator-prey interactions with delays due to juvenile maturation, *SIAM J. Appl. Math.,* **66** (2006), 1050–1079.
[5] R. Driver, Existence and stability of solutions of a delay-differential system, *Arch. Ration. Mech. Anal.*, **10** (1962), 401–426.
[6] B. Ermentrout, *Simulating, Analyzing, and Animating Dynamical Systems: A Guide to XPPAUT for Researchers and Students*, SIAM, 2002.
[7] G. Fan and G. S. K. Wolkowicz, A predator-prey model in the chemostat with time delay, *Int. J. Differ. Equ.*, (2010), Art. ID 287969, 41pp.
[8] J. E. Forde, *Delay Differential Equation Models in Mathematical Biology*, PhD thesis, University of Michigan, 2005.
[9] H. I. Freedman, *Deterministic Mathematical Models in Population Ecology*, Marcel Dekker, New York, 1980.
[10] F. R. Gantmacher, *Applications of the Theory of Matrices*, Trans. J. L. Brenner et al., New York: Interscience, 1959.
[11] A.-M. Ginoux, B. Rossetto and J.-L. Jamet, Chaos in a three-dimensional Volterra-Gause model of predator-prey type, *Internat. J. of Bifur. Chaos Appl. Sci. Engrg.*, **15** (2005), 1689–1708.
[12] S. A. Gourley and Y. Kuang, A stage structured predator-prey model and its dependence on maturation delay and death rate, *J. Math. Biol.,* **49** (2004), 188–200.
[13] J. K. Hale and V. L. S. M., *Introduction to Functional-Differential Equations*, vol. 99 of Applied Mathematical Sciences, Springer-Verlag, New York, 1993.
[14] M. A. Haque, A predator-prey model with discrete time delay considering different growth function of prey, *Adv. Appl. Math. Biosci.*, **2** (2011), 1–16.
[15] A. Hastings and T. Powell, Chaos in a three-species food chain, *Ecology*, **72** (1991), 896–903.
[16] W. M. Hirsch, H. Hanisch and J.-P. Gabriel, Differential equation models of some parasitic infections: methods for the study of asymptotic behavior, *Comm. Pure Appl. Math.*, **38** (1985), 733–753.
[17] Y. Kuang, *Delay Differential Equations with Applications in Population Dynamics*, vol. 191 of Mathematics in Science and Engineering, Academic Press Inc., Boston, MA, 1993.
[18] V. Lakshmikantham and S. Leela, *Differential and Integral Inequalities: Theory and Applications*, vol. 55-I, Academic Press, New York, 1969.
[19] M. Y. Li, X. Lin and H. Wang, Global Hopf branches and multiple limit cycles in a delayed Lotka-Volterra predator-prey model, *Discrete Contin. Dyn. Syst. Ser. B,* **19** (2014), 747–760.
[20] M. C. Mackey and L. Glass, Oscillations and chaos in physiological control, *Science,* **197** (1977), 287–289.
[21] ———, Mackey-Glass equation, *Scholarpedia,* **4** (2009), p. 6908.
[22] MAPLE, *Maplesoft, A Division of Waterloo Maple Inc.*, Waterloo, Ontario, 2017.
[23] MATLAB, *Version 9.5.0 (R2018b)*, The MathWorks Inc., Natick, Massachusetts, 2018.
[24] A. Morozov, S. Petrovskii and B.-L. Li, Bifurcations and chaos in a predator-prey system with the allee effect, *P Roy. Soc. B-Biol. Sci.,* **271** (2004), 1407–1414.
[25] M. L. Rosenzweig, Paradox of enrichment: Destabilization of exploitation ecosystems in ecological time, *Science*, **171** (1971), 385–387.
[26] H. L. Smith, *An Introduction to Delay Differential Equations with Applications to the Life Sciences*, vol. 57 of Texts in Applied Mathematics, Springer, New York, 2011.
[27] H. L. Smith and H. R. Thieme, *Dynamical Systems and Population Persistence*, vol. 118 of Graduate Studies in Mathematics, American Mathematical Society, Providence, RI, 2011.

[28] J. Wang and W. Jiang, Bifurcation and chaos of a delayed predator-prey model with dormancy of predators, *Nonlinear Dynam.*, **69** (2012), 1541–1558.

Appendix A. Proofs.

A.1. **Proof of Proposition 2.1. Proof.** Parts 1 & 2. Assume that $(\phi(t), \psi(t)) \in X$. Since the right hand side of (5) is Lipschitz, there exist $h > 0$ such that solutions exist and are unique for all $t \in [0, h]$. We will show that solutions are bounded and hence do not blow up in finite time. Therefore, by the standard results for existence and uniqueness of solutions for delay differential equations in Driver [5], it will follow that solutions exist and are unique for all $t \geq 0$.

Since $\phi(0) \geqslant 0$, and the face where $x(t) = 0$ is invariant, that $x(t) \geqslant 0$ for all $t \geqslant 0$ follows by uniqueness of solutions in forward time for initial value problems. That $y(t) \geqslant 0$ for all $t > 0$, follows since $y'(t) \geqslant -sy(t)$ for all $t \in [0, \tau]$ and so $y(t) \geqslant 0$ for all $t \in [-\tau, \tau]$. Arguing inductively on $[n\tau, (n+1)\tau]$, $n = 1, 2, \ldots$, it follows that $y(t) \geqslant 0$ for all $t > 0$, where the solution exist.

To show that solutions are bounded above, consider the first equation of (5)

$$\dot{x}(t) = x(t)(1 - x(t)) - y(t)x(t) \leqslant x(t)(1 - x(t)).$$

It is well-known that for the logistic equation $\dot{z}(t) = z(t)\,(1 - z(t))$, given any $\epsilon_0 > 0$, there exists $T > 0$, such that $|z(t)| < 1 + \epsilon_0$ for all $t \geqslant T$. Using a comparison principle (e.g. [18] Theorem 1.4.1, page 15) $x(t) \leqslant z(t)$, and so $0 \leqslant x(t) < 1 + \epsilon_0$ for all $t \geqslant T$.

To prove that $y(t)$ is bounded above, define

$$w(t) = Ye^{-s\tau}x(t - \tau) + y(t). \tag{22}$$

Then

$$\begin{aligned}
\dot{w}(t) &= Ye^{-s\tau}\frac{dx(t-\tau)}{dt} + \frac{dy(t)}{dt}, \\
&= -sy(t) + Ye^{-s\tau}x(t-\tau)\,(1 - x(t-\tau))\,, \\
&= -sw(t) + Ye^{-s\tau}x(t-\tau)\,(s + 1 - x(t-\tau))\,, \\
&\leqslant -sw(t) + \frac{1}{4}Ye^{-s\tau}(s+1)^2,
\end{aligned}$$

since $\left(x(t-\tau) - \frac{s+1}{2}\right)^2 \geqslant 0$ implies that $x(t-\tau)\,(s + 1 - x(t-\tau)) \leqslant \frac{(s+1)^2}{4}$. Therefore, since $z(t) = z(0)e^{-st} + \frac{1}{4s}Ye^{-s\tau}(s+1)^2(1 - e^{-st})$ is the solution of the initial value problem

$$\dot{z}(t) = -sz(t) + \frac{1}{4}Ye^{-s\tau}(s+1)^2, \qquad z(0) = w(0) \geqslant 0,$$

using a comparison principle it follows that $w(t) \leqslant z(t)$ for all $t > 0$. Consequently, by (22), $y(t) \leqslant w(t) \leqslant w(0)e^{-st} + \frac{1}{4s}Ye^{-s\tau}(s+1)^2(1 - e^{-st})$. Therefore, $y(t)$ is bounded.

Part 3. Assume that $(\phi(t), \psi(t)) \in X^0$. Since $\phi(0) > 0$, and the face where $x(t) = 0$ is invariant, it follows that $x(t) > 0$ for all $t \geqslant 0$. Since there exists $\theta \in [-\tau, 0]$ such that $\phi(\theta)\psi(\theta) > 0$, take $T = \tau + \theta$, and note that $0 \leqslant T \leqslant \tau$. Since $y(T) \geqslant 0$, either $y(T) > 0$ or $y(T) = 0$ and by (5), $y'(T) = -sy(T) + Ye^{-s\tau}y(\theta)x(\theta) = 0 + Ye^{-s\tau}\psi(\theta)\phi(\theta) > 0$. In both cases, there exists $\epsilon > 0$ such that $y(t) > 0$ for all $t \in (T, T + \epsilon]$. But this implies that $y'(t) \geqslant -sy(t)$ for all $t \in [-\tau, T + \epsilon + \tau]$. Therefore, $y(t) > 0$ for all $t \in [T + \epsilon, T + \epsilon + \tau]$. By repeating this argument, it follows that $y(t) > 0$ for all $t > T + \epsilon$ for any $\epsilon > 0$. □

A.2. **Proof of Theorem 3.1. Proof.** Part 1. Evaluating (9) at E_0 gives $P(\lambda)|_{E_0} = (\lambda+s)(\lambda-1)=0$, which has two real roots $\lambda=-s$ and $\lambda=1$. Therefore, E_0 is a saddle.

Part 2.(a) Evaluating (9) at E_1 gives $P(\lambda)|_{E_1} = (\lambda+1)(\lambda+s-Ye^{-(s+\lambda)\tau})=0$. One of the roots is $\lambda=-1$. The other roots satisfy $g(\lambda,\tau) := (\lambda+s)e^{(\lambda+s)\tau} = Y$. For any fixed $0 \leqslant \tau < \tau_c$, there is a real root $\lambda(\tau) > 0$, such that $g(\lambda(\tau),\tau) = Y$, since $g(0,\tau) < Y$ and $g(\lambda,\tau) \to \infty$ as $\lambda \to \infty$. Hence, E_1 is unstable.

Part 2.(b) Next assume that $\tau > \tau_c$. We prove that E_1 is globally asymptotically stable. Since $\frac{se^{s\tau}}{Y} > 1$, $\epsilon_0 := \frac{1}{2}\left(\frac{s}{Y}e^{s\tau}-1\right) > 0$, and so by Proposition 2.1, there exists a $T>0$ such that $x(t) < 1+\epsilon_0$ for all $t > T$. Therefore, for all sufficiently large t, $Ye^{-s\tau}x(t-\tau) < Ye^{-s\tau}(1+\epsilon_0) = Ye^{-s\tau}\left(1+\frac{1}{2}\left(\frac{s}{Y}e^{s\tau}-1\right)\right) = \frac{1}{2}Ye^{-s\tau}+\frac{s}{2} < s$, and so the second equation of (5) can be written $\dot{y}(t) = -sy(t)+b(t)y(t-\tau)$, where $b(t) := Ye^{-s\tau}x(t-\tau) < s$. Choosing $\alpha = s/2$ in Kuang [17], (Example 5.1, Chapter 2, page 32), since $b^2(t) < s^2 = 4(s-\alpha)\alpha = 4(s-s/2)(s/2)$, $y(t) \to 0$ as $t \to \infty$. Hence, for any $\epsilon > 0$, there exists T_1 such that $0 < y(t) < \epsilon$ for $t > T_1$. From the first equation of (5), for any $0 < \epsilon < 1$, $x(t)\,(1-x(t)-\epsilon) < \dot{x}(t) < x(t)\,(1-x(t))$. Note that all solutions of $\dot{z}(t) = z(t)(1-z(t))$ converge to $z(t)=1$ and all solutions of $\dot{z}(t) = z(t)(1-z(t)-\epsilon)$ converge to $z(t) = 1-\epsilon$ as $t \to \infty$. By a standard comparison principle, for any solution $x(t)$ of (5), $x(t) \to 1$ as $t \to \infty$. Therefore, E_1 is globally asymptotically stable.

Part 3. Existence of E_+ follows from (7).

Part 3.(a) When $\tau = 0$, model (5) reduces to a well studied model involving only ordinary differential equations. That E_+ is globally asymptotically stable in this case is well known and can easily be proved using phase plane analysis and the Bendixson-negative criterion to rule out periodic solutions.

Part 3.(b) The proof is similar to the approach used in Chapter 5.7 of Smith and Thieme [27]. The predator reproduction number at a constant level of x is given by $\mathcal{R}(x) = \frac{Ye^{-s\tau}}{s}x$. Then, since E_+ exists,

$$\mathcal{R}(1) > 1 \quad \text{and} \quad \mathcal{R}(x_+) = 1. \tag{23}$$

Let, $x^\infty \equiv \limsup_{t\to\infty} x(t)$ and $y^\infty \equiv \limsup_{t\to\infty} y(t)$. Then, we claim

$$x^\infty \geq \frac{se^{s\tau}}{Y}. \tag{24}$$

Suppose not, i.e., that x^∞ is smaller than this minimum. Applying the fluctuation lemma (see Hirsch et. al. [16] or Smith and Thieme [27]) to the y equation in (5), there exists a monotone increasing sequence of times $\{t_n\} \to \infty$ as $n \to \infty$ such that $\dot{y}(t_n) = 0$ and $y(t_n) \to y^\infty$ as $n \to \infty$. Therefore, $0 = \dot{y}(t_n) = -sy(t_n) + Ye^{-s\tau}x(t_n-\tau)y(t_n-\tau)$. Letting $n \to \infty$, we obtain $0 \leq (-s+Ye^{-s\tau}x^\infty)y^\infty$, since $\limsup_{n\to\infty} x(t_n-\tau)y(t_n-\tau) \leq x^\infty y^\infty$. The term in the brackets in this inequality is negative, since we are assuming (24) does not hold. It follows that $y^\infty = 0$. But then, applying the fluctuation lemma to the x equation in (5), it follows that $x^\infty = 1 > \frac{se^{s\tau}}{Y}$, contradicting our assumption that (24) is not satisfied. Hence, (24) holds.

Let $\Phi : \mathbb{R}_+ \times X \to X$ denote the semiflow generated by model (5). Consider the function $\rho : X \to \mathbb{R}_+$, defined for $(\phi(t),\psi(t)) \in X^0$ by $\rho((\phi,\psi)) = \phi(0)$ so that $\rho(\Phi(t,(\phi,\psi))) = x(t)$. By part 3 of Proposition 2.1, $\rho((\phi,\psi))) > 0$ implies that $\rho(\Phi(t,(\phi,\psi))) > 0$ for all $t \geq 0$. Therefore, the semi-flow is uniformly weakly ρ-persistent. By a similar argument to that given in Theorem 5.29 of [27] together with Proposition 2.1, Φ is a continuous semiflow that has a compact attractor of

bounded sets. Therefore, ϕ is uniformly ρ-persistent by Theorem 5.2 of [27], and hence there exists $\epsilon_1 > 0$ such that $x_\infty \equiv \liminf_{t\to\infty} x(t) \geq \epsilon_1$, for all solutions with $x(0) > 0$.

Before, we show that if $(\phi, \psi) \in X^0$, there exists $\epsilon_2 > 0$ such that $\liminf_{t\to\infty} y(t) > \epsilon_2$, we use Laplace transforms to show that if $(\phi, \psi) \in X^0$, then $\mathcal{R}(x_\infty) \leq 1$. We denote the Laplace transform of a function $f(t)$ as $\widehat{f}(\lambda) = \int_0^\infty e^{-\lambda t} f(t)\, dt$, and note that the Laplace transform of $y(t)$ exists for all $\lambda > 0$, since $y(t)$ is bounded by Proposition 2.1. Taking the Laplace transform on both sides of the y equation of (5) and simplifying we obtain:

$$(\lambda + s)\widehat{y}(\lambda) = y(0) + Ye^{-(s+\lambda)\tau}\widehat{xy}(\lambda) + Ye^{-(s+\lambda)\tau}\int_{-\tau}^{0} e^{-\lambda\tau} x(t)y(t)\, dt.$$

There exists $\delta > 0$ such that $x(t) \geq (x_\infty - \delta)$ for all $t \geq 0$, and so $\widehat{xy}(\lambda) \geq (x_\infty - \delta)\widehat{y}(\lambda)$.

$$(\lambda + s)\widehat{y}(\lambda) \geq Ye^{-(s+\lambda)\tau}(x_\infty - \delta)\widehat{y}(\lambda).$$

By part 3 of Proposition 2.1, $y(t) > 0$ for all sufficiently large t, and hence $\widehat{y}(\lambda) > 0$, we can divide by $\widehat{y}(\lambda)$ to obtain

$$(\lambda + s) \geq Ye^{-(s+\lambda)\tau}(x_\infty - \delta).$$

After a shift of time, if necessary, we can take the limit as $\delta, \lambda \to 0^+$ to obtain $s \geq Ye^{-s\tau}x_\infty$. This is equivalent to

$$\mathcal{R}(x_\infty) \leq 1. \tag{25}$$

Define $\rho : X \to \mathbb{R}_+$ by $\rho((\phi, \psi)) = \min\{\phi(0), \psi(0)\}$.
Then, $\rho(\Phi(t, (\phi, \psi))) = \min\{x(t), y(t)\}$. Suppose $(\phi, \psi) \in X^0$ and $y(t)$ is not uniformly persistent. By part 3 of Proposition 2.1, shifting time if necessary, there is no loss of generality if we assume that $\psi(0) = y(0) > 0$. Therefore, $\rho(\Phi(t, (\phi, \psi))) > 0$ for all $t \geq 0$. Since by Proposition 2.1, Φ has a compact attractor of bounded sets, by Theorem 5.2 in [27] we need only show that Φ is uniformly weakly ρ-persistent. Suppose not. Recall that we have already shown that $x_\infty > \epsilon_1 > 0$. Take any $\epsilon \in (0, \epsilon_1)$. Then, there exists a solution with $x(0) > 0$ and $y(0) > 0$ such that $y^\infty < \epsilon$. Apply the fluctuation lemma to the x equation of (5). Therefore, $0 > x_\infty(1 - x_\infty - \epsilon)$. Taking $\epsilon > 0$ sufficiently small, since $\mathcal{R}(1) > 1$ by (23) and $\mathcal{R}(x)$ is increasing, it follows that $\mathcal{R}(x_\infty) > 1$, contradicting (25). □

A.3. **Proof of Lemma 3.2: Roots of the characteristic equation cannot bifurcate in from infinity. Proof.** In Kuang [17] (Theorem 1.4, Chapter 3, page 66), taking $n = 2$ and $g(\lambda, \tau) = p(\tau)\lambda + (q\lambda + c(\tau))e^{-\lambda\tau} + \alpha(\tau)$, since

$$\limsup_{\mathrm{Re}\lambda > 0, |\lambda|\to\infty} |\lambda^{-2} g(\lambda, \tau)| = 0 < 1,$$

no root of (10) with positive real part can enter from infinity as τ increases from 0. Since, when $\tau = 0$ all roots have negative real parts, the result follows. □

A.4. **Proof of Theorem 3.3. Proof.** Using the quadratic formula to solve for ω^2 in (13), the roots must satisfy

$$\omega_\pm^2 = \frac{1}{2}\left(q^2 - p^2(\tau) + 2\alpha(\tau) \pm \sqrt{(q^2 - p^2(\tau) + 2\alpha(\tau))^2 - 4\left(\alpha^2(\tau) - c^2(\tau)\right)}\right).$$

Since

$$q^2 - p^2(\tau) + 2\alpha(\tau) = s^2 - s^2\left(1 + \frac{e^{s\tau}}{Y}\right)^2 + 2\frac{s^2 e^{s\tau}}{Y} = -\left(\frac{se^{s\tau}}{Y}\right)^2 < 0,$$

ω_-^2 is either complex or negative for any $\tau \geqslant 0$, and ω_+^2 is positive, if, and only if,

$$(\alpha^2(\tau) - c^2(\tau)) = -3s^2\left(\frac{se^{s\tau}}{Y} - \frac{1}{3}\right)\left(\frac{se^{s\tau}}{Y} - 1\right) < 0.$$

This is the case, if, and only if, $\frac{se^{s\tau}}{Y} < \frac{1}{3}$ or $\frac{se^{s\tau}}{Y} > 1$. However, E_+ only exists when $x_+(\tau) = \frac{se^{s\tau}}{Y} < 1$. Therefore, a real positive root exists if, and only if, $x_+(\tau) = \frac{se^{s\tau}}{Y} < \frac{1}{3}$. This implies that $\tau < \tau^*$. Hence, for $\tau \in [0, \tau^*)$, a real positive root $\omega_+(\tau)$ exists, and is defined explicitly by (16).

If $\tau = \tau^*$, then $\omega_+(\tau) = 0$, and if $\tau > \tau^*$, then either $\omega_+(\tau)$ is not real or E_+ does not exist. □

A.5. Properties of the functions $h_1(\omega, \tau)$ and $h_2(\omega, \tau)$ defined in (17).

Lemma A.1. *Assume that E_+ exists and that $\frac{s}{Y} < \frac{1}{3}$.*

1. *If $\tau \in [0, \tau^*]$, then $h_1^2(\omega_+(\tau), \tau) + h_2^2(\omega_+(\tau), \tau) = 1$.*
2. *$h_1(\omega_+(\tau^*), \tau^*) = 0$. If $0 \leqslant \tau < \tau^*$, then $h_1(\omega_+(\tau), \tau) > 0$.*
3. *$h_2(\omega_+(\tau^*), \tau^*) = -1$. If $0 \leqslant \tau < \tau^*$, then $-1 < h_2(\omega_+(\tau), \tau) < 1$.*

Proof. Part 1. Since $h_1(\omega_+(\tau), \tau)$ is equal to the right-hand side of (12a), and $h_2(\omega_+(\tau), \tau)$ is equal to the right-hand side of (12b), where $\omega = \omega_+(\tau)$ satisfies (13), it follows that $h_1^2(\omega_+(\tau), \tau) + h_2^2(\omega_+(\tau), \tau) = 1$.

Part 2. By Theorem 3.3, $\omega_+(\tau^*) = 0$, and so $h_1(\omega_+(\tau^*), \tau^*) = 0$. Since for $t \in [0, \tau^*)$, $x_+(\tau) < \frac{1}{3}$ and by Theorem 3.3, $\omega_+(\tau) > 0$, it follows that the denominator of $h_1(\tau, \omega_+(\tau))$ is always positive. Hence, $h_1(\omega_+(\tau), \tau) > 0$, if, and only if,

$$\begin{aligned} 0 &< s(1 - x_+(\tau)) + x_+(\tau)(1 - 2x_+(\tau)) - \omega_+^2(\tau) \\ &= s(1 - x_+(\tau)) + x_+(\tau)(1 - 2x_+(\tau)) \\ &\quad -\frac{1}{2}\left(-x_+^2(\tau) + \sqrt{x_+^4(\tau) + 4s^2(3x_+(\tau) - 1)(x_+(\tau) - 1)}\right). \end{aligned}$$

This is equivalent to,

$$\frac{1}{2}\sqrt{x_+^4(\tau) + 4s^2(3x_+(\tau) - 1)(x_+(\tau) - 1)} < s(1 - x_+(\tau)) + x_+(\tau)(1 - \frac{3}{2}x_+(\tau)).$$

Since $x_+(\tau) < \frac{1}{3}$, both sides of the above inequality are positive. Squaring, both sides yields,

$$\begin{aligned} &\frac{1}{4}\left(x_+^4(\tau) + 4s^2(1 - 3x_+(\tau))(1 - x_+(\tau))\right) \\ &\quad < s^2(1 - x_+(\tau))^2 + x_+^2(\tau)(1 - \frac{3}{2}x_+(\tau))^2 \\ &\qquad + \quad 2sx_+(\tau)(1 - x_+(\tau)(1 - \frac{3}{2}x_+(\tau)). \end{aligned}$$

But this is equivalent to,

$$\begin{aligned} 0 &< 2s^2 x_+(\tau)(1 - x_+(\tau)) + x_+^2(\tau)(1 - 2x_+(\tau))(1 - x_+(\tau)) \\ &\quad + \quad 2sx_+(\tau)(1 - x_+(\tau)(1 - \frac{3}{2}x_+(\tau)). \end{aligned}$$

This last inequality is satisfied, since by part 2 of Theorem 3.3, $x_+(\tau) < \frac{1}{3}$, and so $h_1(\omega_+(\tau), \tau) > 0$ for $\tau \in [0, \tau^*)$.

Part 3. That $h_2((\omega_+(\tau^*), \tau^*) = -1$, follows from a straightforward calculation, after substituting $\omega_+(\tau^*) = 0$ and $x_+(\tau^*) = \frac{1}{3}$ in (17b). For $\tau \in [0, \tau^*)$, the result follows immediately, by parts 1 and 2. □

A.6. **Proof of Theorem 3.4. Proof.** Assume that $\bar{\tau} \in (0, \tau^*)$. By Remark 3, (10) has a pair of pure imaginary eigenvalues, if and only if, $\bar{\tau} = \tau_n^j \in (0, \tau^*)$, for some $n \geqslant 0$, $0 \leqslant j \leqslant j_n$. Since a necessary condition for a root of (10) to exist is that (13) holds, and hence $\omega(\bar{\tau}) = \omega_+(\bar{\tau})$ given by (16), there can be at most one pair of pure imaginary roots for each such $\tau = \bar{\tau}$, and hence if any such roots exist, they are simple, and no other root of (10) is an integer multiple.

In Beretta and Kuang, [3] (Theorem 4.1, equation (4.1) p.1157), it is shown that

$$\operatorname{sign}\left(\frac{\mathrm{d}}{\mathrm{d}\tau}\mathrm{Re}(\lambda(\tau))\right)\Big|_{\tau=\tau_{nj}} = \operatorname{sign}\left(\frac{\mathrm{d}}{\mathrm{d}\tau}\left[\frac{\tau\omega_+(\tau) - (\theta(\tau) + 2n\pi)}{\omega_+(\tau)}\right]\right)\Big|_{\tau=\tau_n^j}.$$

After differentiating, and noting that $\omega_+(\tau_n^j) > 0$ and $\tau_n^j\omega_+(\tau_n^j) - (\theta(\tau_n^j) + 2n\pi) = 0$, it is easy to see that the term on the right has the same sign as $\left(\frac{\mathrm{d}}{\mathrm{d}\tau}\left[\tau\omega_+(\tau) - (\theta(\tau) + 2n\pi)\right]\right)|_{\tau=\tau_n^j}$. It follows that transversality holds whenever the graphs of $\tau\omega_+(\tau)$ and $\theta(\tau)$ have different slopes at τ_n^j. □

A.7. **Proof of Corollary 3.5. Proof.** Parts 1, 2 and 3 follow immediately from Theorem 3.4, since for $\tau \in [0, \tau^*]$, both curves are continuous, by part 3 of Lemma A.1 and Remark 4, $\theta(\tau) \in (0, \pi)$, and $\tau\omega_+(\tau) \geqslant 0$ with equality for $\tau = 0$ and $\tau = \tau^*$. (See Figure 1 for typical examples.)

Next consider local stability of E_+ when it exists, i.e. $\tau \in [0, \tau_c)$. By part 3(a) of Theorem 3.1, E_+ is globally asymptotically stable when $\tau = 0$. By Lemma 3.2, E_+ can only change stability for $0 \leqslant \tau < \tau_c$, if a pair of roots cross the imaginary axis. As τ increases from 0, by part 3, the first possible such crossing occurs for $\tau = \tau_0^1$. Hence, E_+ is locally asymptotically stable for $\tau \in [0, \tau_0^1)$. When $\tau = \tau_c$, E_+ and E_1 coalesce, and by part 2(b) of Theorem 3.1, E_1 is globally asymptotically stable for $\tau > \tau_c$. Since again by Lemma 3.2, E_+ can only change stability for $0 \leqslant \tau < \tau_c$, if a pair of roots cross the imaginary axis, and $\tau_0^{j_0}$ is the last possible such crossing, E_+ must be locally asymptotically stable for $\tau \in (\tau_0^{j_0}, \tau_c)$. □

Received March 2020; revised July 2020.

E-mail address: fan_guihong@columbusstate.edu
E-mail address: wolkowic@mcmaster.ca